PLOS ONE

RESEARCH ARTICLE

Apoptosis inhibitor of macrophage depletion decreased M1 macrophage accumulation and the incidence of cardiac rupture after myocardial infarction in mice

Shohei Ishikawa[1], Takahisa Noma[1], Hai Ying Fu[2], Takashi Matsuzaki[1], Makoto Ishizawa[1], Kaori Ishikawa[1], Kazushi Murakami[1], Naoki Nishimoto[3], Akira Nishiyama[4], Tetsuo Minamino[1]*

1 Department of Cardiorenal and Cerebrovascular Medicine, Faculty of Medicine, Kagawa University, Kagawa, Japan, **2** Department of Cardiovascular Medicine, Osaka University Graduate School of Medicine, Suita, Osaka, Japan, **3** Clinical Research Support Center, Kagawa University Hospital, Kagawa, Japan, **4** Department of Pharmacology, Faculty of Medicine, Kagawa University, Kagawa, Japan

* minamino@med.kagawa-u.ac.jp

OPEN ACCESS

Citation: Ishikawa S, Noma T, Fu HY, Matsuzaki T, Ishizawa M, Ishikawa K, et al. (2017) Apoptosis inhibitor of macrophage depletion decreased M1 macrophage accumulation and the incidence of cardiac rupture after myocardial infarction in mice. PLoS ONE 12(11): e0187894. https://doi.org/10.1371/journal.pone.0187894

Editor: Michael Bader, Max Delbruck Centrum fur Molekulare Medizin Berlin Buch, GERMANY

Received: February 20, 2017

Accepted: October 27, 2017

Published: November 9, 2017

Data Availability Statement: All relevant data are within the paper.

Funding: This research was supported by a Core Research for Evolutional Medical Science and Technology grant funded by the Agency for Medical Research and Development (AMED-CREST) (to Akira Nishiyama) and Grants-in-aid from the Ministry of Education, Culture, Sports, Science and Technology, Japan (to Tetsuo Minamino).

Abstract

Background

Cardiac rupture is an important cause of death in the acute phase after myocardial infarction (MI). Macrophages play a pivotal role in cardiac remodeling after MI. Apoptosis inhibitor of macrophage (AIM) is secreted specifically by macrophages and contributes to macrophage accumulation in inflamed tissue by maintaining survival and recruiting macrophages. In this study, we evaluated the role of AIM in macrophage accumulation in the infarcted myocardium and cardiac rupture after MI.

Methods and results

Wild-type (WT) and AIM$^{-/-}$ mice underwent permanent left coronary artery ligation and were followed-up for 7 days. Macrophage accumulation and phenotypes (M1 pro-inflammatory macrophage or M2 anti-inflammatory macrophage) were evaluated by immunohistological analysis and RT-PCR. Matrix metalloproteinase (MMP) activity levels were measured by gelatin zymography. The survival rate was significantly higher (81.1% vs. 48.2%, $P<0.05$), and the cardiac rupture rate was significantly lower in AIM$^{-/-}$ mice than in WT mice (10.8% vs. 31.5%, $P<0.05$). The number of M1 macrophages and the expression levels of M1 markers (iNOS and IL-6) in the infarcted myocardium were significantly lower in AIM$^{-/-}$ mice than in WT mice. In contrast, there was no difference in the number of M2 macrophages and the expression of M2 markers (Arg-1, CD206 and TGF-β1) between the two groups. The ratio of apoptotic macrophages in the total macrophages was significantly higher in AIM$^{-/-}$ mice than in WT mice, although MCP-1 expression did not differ between the two groups. MMP-2 and 9 activity levels in the infarcted myocardium were significantly lower in AIM$^{-/-}$ mice than in WT mice.

Competing interests: The authors have declared that no competing interests exist.

Conclusions

These findings suggest that AIM depletion decreases the levels of M1 macrophages, which are a potent source of MMP-2 and 9, in the infarcted myocardium in the acute phase after MI by promoting macrophage apoptosis, and leads to a decrease in the incidence of cardiac rupture and improvements in survival rates.

Introduction

Acute myocardial infarction (AMI) is a major cause of death in developed nations [1,2]. Current therapies, including percutaneous coronary intervention (PCI) and pharmaceutical treatments, are effective in reducing mortality in patients with AMI. Although AMI-related mortality has decreased to one-third of its previous levels over the past three decades in Japan [3], the mortality of cardiac rupture due to MI remains high (about 30–80%) [4, 5]. Thus, it is a world-wide unmet clinical need to elucidate the mechanisms of cardiac rupture after AMI.

Macrophages play a pivotal role in cardiac remodeling after MI [6]. Although macrophage-induced inflammatory responses are essential for cardiac repair, they also contribute to the development of cardiac rupture [7]. Macrophages are grouped into the following two phenotypes: a pro-inflammatory (M1) and an anti-inflammatory (M2) phenotypes [8]. The main functions of M1 macrophages include phagocytosis of cellular debris at sites of myocardial damage, secretion of inflammatory cytokines and reorganization of tissue matrices by producing metalloproteinases (MMPs) in the acute phase after MI [9, 10]. In contrast, M2 macrophages facilitate resolution of inflammation and regeneration by promoting myofibroblast accumulation, collagen deposition, and angiogenesis [11].

It was reported that macrophage accumulation in the infarcted myocardium might be involved in cardiac rupture [12, 13], whereas M2 macrophages have been reported to have an inhibitory effect on cardiac rupture [14, 15]. Therefore, it is assumed M1 macrophages in the infarcted myocardium might contribute to cardiac rupture. However, the precise roles of M1 and M2 macrophages in the pathogenesis of cardiac rupture have not been fully elucidated.

Apoptosis inhibitor of macrophage (AIM) is a macrophage-specific secreted protein [16]. AIM appears to increase resistance to multiple initiators of apoptosis, including steroids, irradiation, Fas/CD95, and infection [17, 18]. Furthermore, AIM influences M1 macrophage recruitment to inflammatory tissues by facilitating monocyte chemoattractant protein 1 (MCP-1) expression [19, 20].

Therefore, we hypothesized that AIM may contribute to M1 macrophage accumulation in the infarcted myocardium in the acute phase after MI, which may lead to augmentation of inflammatory response and cardiac rupture, by inhibiting macrophage apoptosis and promoting macrophage recruitment.

In this study, we evaluated the role of AIM in cardiac rupture, M1 and M2 macrophage accumulation and MMP activity levels in the infarcted myocardium after MI in mice.

Materials and methods

Ethic statement

This study was carried out in strict accordance with the recommendations in the Guide for the Care and Use of Laboratory Animals of the National Institutes of Health. The protocol was approved by the Animal Care and Use Committee for Kagawa University (Permit Number:

125–2). Isoflurane anesthesia was used to reduce the suffering and distress of the mice during any procedure that was potentially painful or stressful.

Animals

$AIM^{-/-}$ mice were obtained from Toru Miyazaki at Tokyo University [17]. $AIM^{-/-}$ mice were backcrossed with C57BL/6 mice for at least 15 generations before being used for the experiments described herein. Eight- to ten-week-old male $AIM^{-/-}$ and C57BL/6J wild-type (WT) mice were used in the present study.

Infarct model

MIs were induced in the above mice as described previously [21]. Briefly, the mice were anesthetized with isoflurane, intubated, and put on a mechanical small-animal ventilator. The chest wall was shaved, and a left thoracotomy was performed at the second left intercostal space. The pericardial sac was opened, and the left coronary artery was permanently ligated with a monofilament nylon 8–0 suture at the site of its emergence from the left atrium. Sham-operated mice in both groups underwent the same procedure but did not undergo coronary artery ligation. Blood pressures and pulse rates were measured by the tail-cuff method under 0.5% isoflurane anesthesia before surgery.

Experimental protocol

Survival analysis was performed in WT (n = 54) and $AIM^{-/-}$ (n = 37) mice. The mice were followed up for 7 days after surgery. The mice health and behavior were observed every day during the experimental procedure and there were no unexpected deaths among these mice. All dead mice were examined for the presence of MI and the cause of death by autopsy. Cardiac rupture was confirmed based on the presence of blood coagulation around the pericardial sac and in the chest cavity, and heart failure was diagnosed based on the presence of lung congestion with pleural effusions. Day 1 was defined as 24–48 hours after surgery, and mice that died within 24 hours after surgery (day 0) and mice that were found to have small infarcts (grossly $<$50% of the left ventricular circumference at the mid-papillary level) at the time of sacrifice or autopsy were excluded from the data analysis. Furthermore, separate groups of mice were used for echocardiography or hemodynamic analysis. Echocardiography was performed before and 3, 7 days after MI (n = 16–34 per group). Hemodynamic analysis was performed at 3 days after MI or sham surgery (n = 3–7 per group). After these analyses, mice were sacrificed for histopathological analysis including immunoblotting, immunohistochemistry and real-time PCR. All mice were deeply anesthetized by isoflurane and sacrificed by cervical dislocation.

In order to reduce the suffering of mice, we set humane endpoints to decide when to euthanize the mice. Humane endpoints in the study included decreased activity with respiratory distress, inability to remain upright and seizures.

Echocardiography and hemodynamic analysis

Transthoracic ultrasound cardiography (UCG) was performed using an echocardiographic system (22-MHz linear transducer; LOGIQ e R6 (GE Healthcare, Amersham, UK). Left ventricular end-diastolic and end-systolic diameter (LVDd and LVDs, respectively) were measured in the M-mode at the level of the papillary muscle, and the heart rate was calculated from the RR interval. Fractional shortening (FS) was calculated as FS (%) = 100 × [(LVDd—LVDs)/LVDd]. Hemodynamic analysis was performed using a 1.4-F micromanometer-tipped catheter (Millar Instruments, Houston, TX, USA) as described [22]. Left ventricular systolic

pressure (LVSP) and left ventricular end-diastolic pressure (LVEDP) were measured under light isoflurane anesthesia (0.5%). Measurement of these parameters was performed after intraventricular pressure and HR became stable.

Morphometric analysis

Heart tissue was fixed in formalin, embedded in paraffin, and cut into 2-μm-thick sections. Sections were stained with picrosirius red to determine the infarct size. Infarct size was calculated as infarct circumference dived by LV circumference as described previously [23].

Western blot analysis

Western blot analysis was performed as described previously [24, 25]. Proteins extracted from the infarcted myocardium were subjected to 8% polyacrylamide gel electrophoresis and then transferred onto polyvinylidene difluoride membranes. The membranes were then probed using primary antibodies against AIM (1:1000, Trans Genic Inc., Fukuoka, Japan), MMP-2 (1:2000, Abcam, Cambridge, UK) and MMP-9 (1:1000, Abcam, Cambridge, UK).

Histological analysis

Immunohistochemistry analysis was performed as described previously [22]. Briefly, paraffin sections were stained with rat anti-mouse MAC-3 (1:300, BD Biosciences, Franklin Lakes, NJ, USA) for total macrophages and incubated overnight at 4˚C. The following day, the sections were incubated with TaKaRa POD conjugate anti-rat for mouse tissue (Takara Bio Inc., Otsu, Japan) in place of a biotin-labeled secondary antibody, and staining was immediately visualized with DAB (Takara Bio Inc., Otsu, Japan). The number of macrophages was assessed by counting the number of MAC-3-positive cells in the infarcted myocardium at 3 days after MI. To evaluate the phenotype of macrophages, immunofluorescence analysis was performed as described previously [26]. Staining with rabbit anti-mouse iNOS antibody (1:25, Abcam, Cambridge, UK) for M1 macrophages and rabbit anti-mouse CD206 (1:1000, Abcam, Cambridge, UK) for M2 macrophages was performed followed by visualization with anti-rabbit IgG Alexa Fluor 555 (1:1000 Cell signaling, Danvers, MA, USA). Nuclei were stained with mounting medium containing the DAPI fluorescent dye (Wako Pure Chemical Industries Ltd., Osaka, Japan). Apoptotic cells in the infarcted myocardium were detected by Tdt-mediated dUTP nick-end labeling (TUNEL) after proteinase K treatment using the apoptosis detection kit (Takara Bio Inc., Otsu, Japan). Apoptosis of macrophages was evaluated by using mirror sections as described previously [26].

Real-time PCR

Gene expression was evaluated in the infarct zones of hearts collected at 3 days after MI or sham surgery. Real-time quantitative PCR was performed as described previously [27]. The specific primers used in the present study are shown in Table 1. The relative expression levels of each gene were normalized to Hprt [28] and were quantified using the ΔCT (Ct_{Target}−-Ct_{Hprt}) method, and the fold changes in gene expression compared with sham-operated WT mice were quantified using the $2^{-\Delta\Delta CT}$ method [29].

Gelatin zymography

MMP-2 and 9 activity levels in the infarcted myocardium were measured by gelatin zymography at 7 days after MI. Zymography was performed as described previously [30]. Briefly, equal amounts (10 μg) of protein were loaded onto each lane of a 0.15% gelatin zymogram gel. After

Table 1. Primers used for real-time PCR in this study.

Gene		Sequence
IL-6	forward	TGATGGATGCTACCAAACTGG
	reverse	TTCATGTACTCCAGGTAGCTATGG
iNOS	forward	TGGCCACCAAGCTGAACT
	reverse	TTCATGATAACGTTTCTGGCTCT
IL-1β	forward	AGTTGACGGACCCCAAAAG
	reverse	AGCTGGATGCTCTCATCAGG
CD206	forward	CCACAGCATTGAGGAGTTTG
	reverse	ACAGCTCATCATTTGGCTCA
Arg-1	forward	GAATCTGCATGGGCAACC
	reverse	GAATCCTGGTACATCTGGGAAC
TGF-β1	forward	TGGAGCAACATGTGGAACTC
	reverse	GTCAGCAGCCGGTTACCA
MCP-1	forward	CATCCACGTGTTGGCTCA
	reverse	GATCATCTTGCTGGTGAATGAGT
Hprt	forward	TCCTCCTCAGACCGCTTTT
	reverse	AACCTGGTTCATCATCGCTAA

iNOS, inducible NO synthase; Arg-1, arginase-1; TGF-β1, transforming growth factor-β1; MCP-1, monocyte chemoattractant protein-1; Hprt, hypoxanthine phosphoribosyltransferase.

https://doi.org/10.1371/journal.pone.0187894.t001

electrophoresis, the gel was incubated with developing buffer (50 mM Tris-HCl; 200 mM NaCl; and 5 mM $CaCl_2$, pH 7.5) for 48 hours at 37˚C and stained with Coomassie blue (Bio Rad, USA). Gelatinolytic band intensity was quantified using ImageJ software (Wayne Rasband, National Institutes of Health, USA).

Statistical analysis

All data are expressed as the mean ± SEM. Survival analysis was performed using the Kaplan-Meier method, and survival curves were compared using the log-rank test. The significance of the differences in the incidence of cardiac rupture between $AIM^{-/-}$ and WT mice after MI was assessed by Fisher's exact test. Comparisons between 2 groups were performed with Student's *t* test (for normally distributed data) or the Mann-Whitney U test (for non-normally distributed data). When more than 2 groups were analyzed, one-way ANOVA with Bonferroni post-hoc test was used. $P<0.05$ was considered significant. All statistical analyses were performed with the SPSS 21.0 statistical software package for Windows (SPSS Inc, Chicago, IL, USA).

Results

Cardiac rupture and the infarct size in WT and $AIM^{-/-}$ mice after MI

AIM protein was detected in the infarcted myocardium of WT mice, but not $AIM^{-/-}$ mice (S1 Fig). Compared to the sham-operated myocardium, AIM protein levels increased in the infarcted myocardium in WT mice. Fifty-four WT mice and 37 $AIM^{-/-}$ mice were used in this survival rate study and 26 WT mice and 30 $AIM^{-/-}$ mice survived to terminal. $AIM^{-/-}$ mice had a significantly higher 7-day post-MI survival rate than WT mice (81.1% vs. 48.2%, $P<0.05$; Fig 1). Seventeen WT mice and four $AIM^{-/-}$ mice suffered fatal rupture of the left ventricular wall between 3 and 6 days after MI (Fig 2A) and the occurrence of cardiac rupture peaked at 4 days after MI in both groups. The rate of cardiac rupture-associated mortality within 6 days

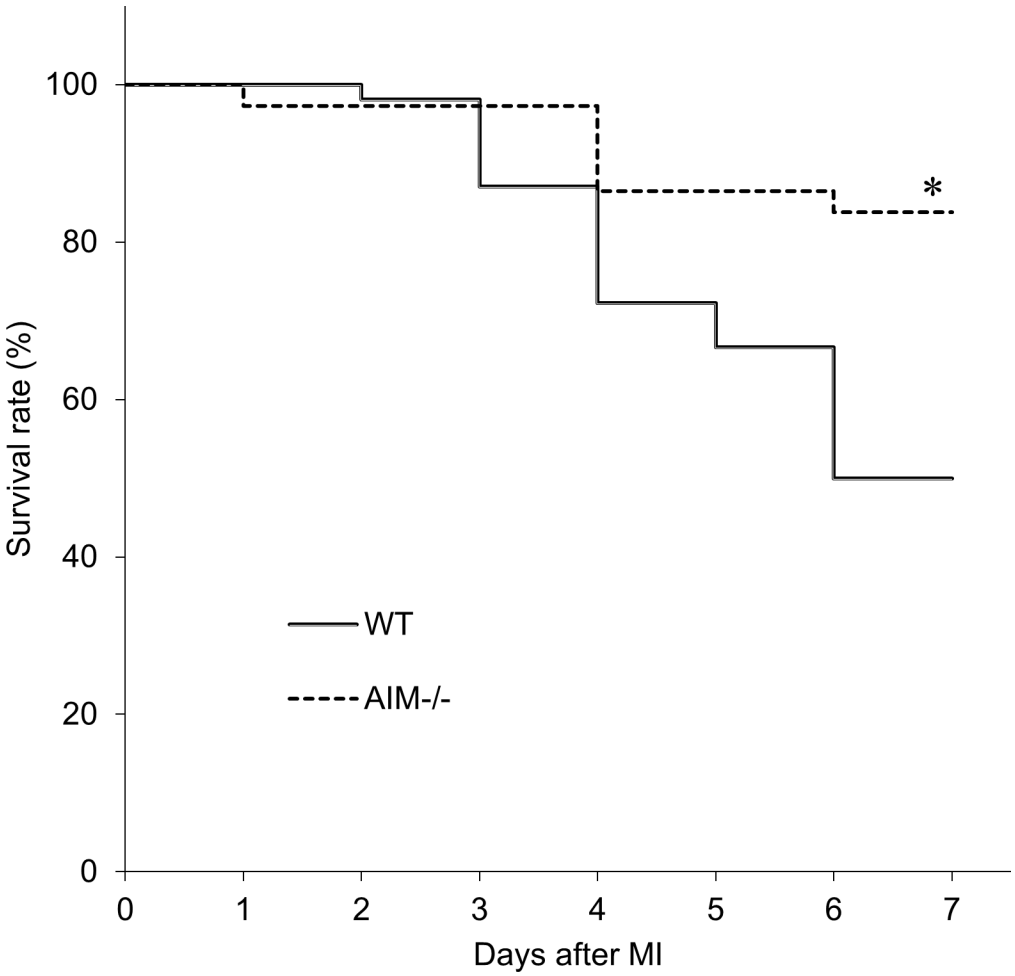

Fig 1. Survival rates for the WT and AIM$^{-/-}$ groups after MI. Kaplan-Meier survival curves for the WT and AIM$^{-/-}$ groups after MI. *P<0.05 compared with WT mice.

https://doi.org/10.1371/journal.pone.0187894.g001

after MI was significantly higher in WT mice than in AIM$^{-/-}$ mice (31.5% vs. 10.8%, P<0.05; Fig 2B).

The infarct size determined by the morphometric analysis of picrosirius red stained left ventricular cross-sections at 7 days after MI was comparable (65.7 ± 1.6% vs. 69.2 ± 2.3%, P = ns (not significant)) between WT and AIM$^{-/-}$ mice (S2 Fig).

Echocardiographic and hemodynamic data for the WT and AIM$^{-/-}$ groups before and 3, 7 days after MI

Before coronary artery ligation, there were no significant differences in systolic blood pressure (93.4 mmHg vs. 92.8 mmHg, P = ns) or heart rate (558 bpm vs. 563 bpm, P = ns), echocardiographic parameters such as LVDd, LVDs and FS between the WT and AIM$^{-/-}$ groups.

Following MI, LVDd and LVDs were increased, and FS was decreased in WT and AIM$^{-/-}$ mice. However, there were no significant differences in these parameters between WT and AIM$^{-/-}$ mice (Table 2). LVSP and LVEDP measured by hemodynamic analysis at 3 days after MI were also comparable between WT and AIM$^{-/-}$ groups (Table 3).

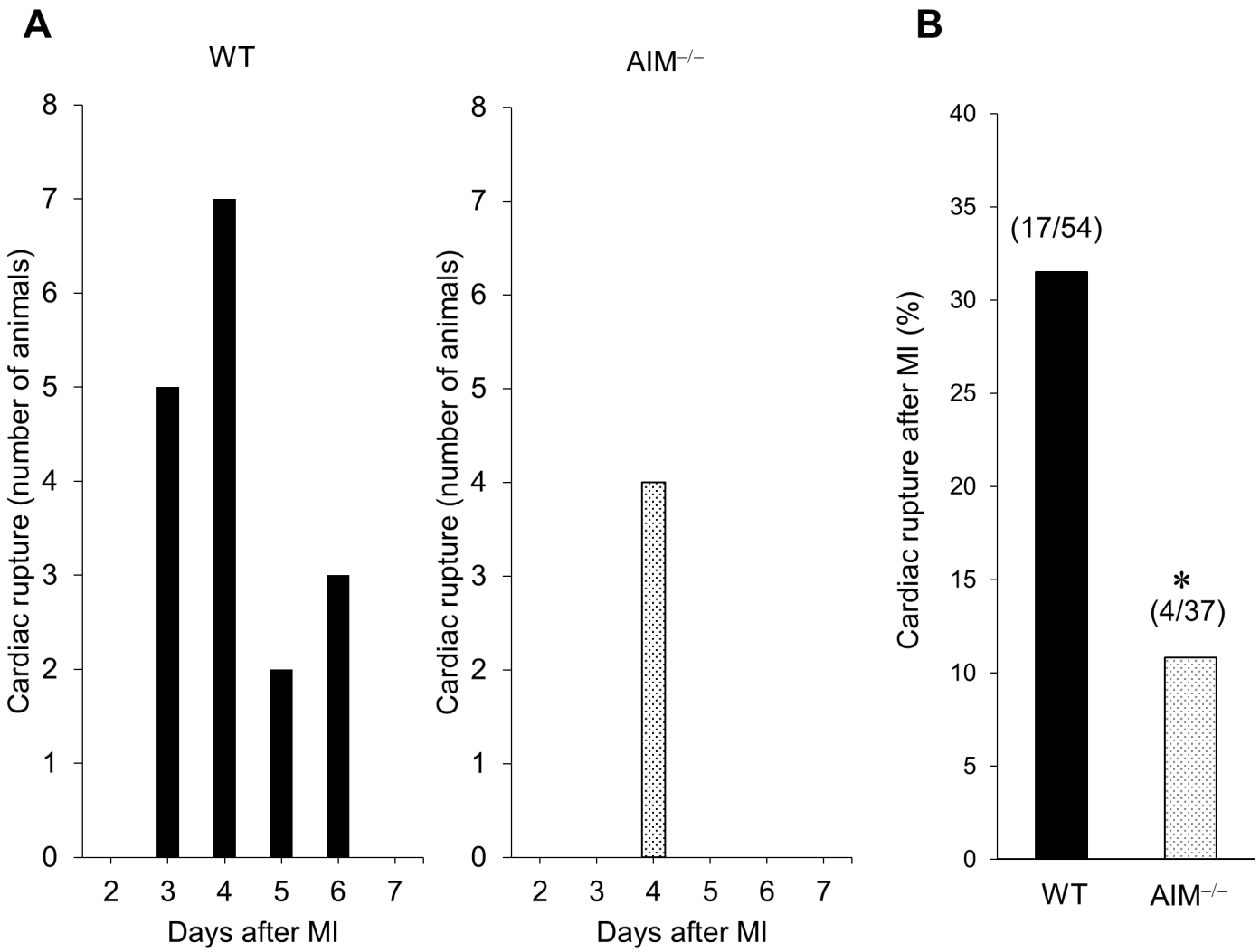

Fig 2. Cardiac rupture in WT and AIM$^{-/-}$ mice after MI. The number of animals that died of cardiac rupture in the WT and AIM$^{-/-}$ groups **(A)**, and the percentages of mice in each group that suffered cardiac rupture after MI **(B)**. * $P<0.05$ compared with WT mice.

https://doi.org/10.1371/journal.pone.0187894.g002

Table 2. Echocardiographic data for the WT and AIM$^{-/-}$ groups before and 3, 7 days after MI.

	Before MI		3 days after MI		7 days after MI	
	WT (n = 31)	AIM$^{-/-}$ (n = 34)	WT (n = 17)	AIM$^{-/-}$ (n = 18)	WT (n = 16)	AIM$^{-/-}$ (n = 17)
HR (bpm)	431.1±8.5	444.5±6.1	492.2±11.0	490.0±7.9	485.2±11.0	477.6±7.8
LVDd (mm)	3.37±0.03	3.47±0.05	4.81±0.07*	4.99±0.06*	5.82±0.12*	5.55±0.07*
LVDs (mm)	1.73±0.03	1.80±0.04	4.33±0.08*	4.47±0.09*	5.34±0.14*	5.00±0.10*
FS (%)	48.6±0.8	48.2±0.7	10.1±0.7*	10.4±0.7*	8.3±0.8*	10.1±0.8*

LVDd, left ventricular end-diastolic diameter; LVDs, left ventricular end-systolic diameter; FS, Fractional shortening. Values are means ± SEM.
*P<0.05 compared with the WT mice before MI.

https://doi.org/10.1371/journal.pone.0187894.t002

Table 3. Hemodynamic data for the WT and AIM$^{-/-}$ groups at 3 days after MI.

	Sham		MI	
	WT (n = 3)	AIM$^{-/-}$ (n = 3)	WT (n = 5)	AIM$^{-/-}$ (n = 7)
Heart rate (bpm)	400.7±3.3	400.7±6.5	401.7±8.9	391.1±7.5
LVSP (mmHg)	105.6±5.4	108.4±5.4	89.4±3.9	89.3±3.4
LVEDP (mmHg)	5.2±0.7	5.8±0.7	12.9±0.9*	13.7±1.1*

LVSP, left ventricular systolic pressure; LVEDP, left ventricular end-diastolic pressure. Values are means ± SEM.

*P<0.05 compared with sham-operated WT mice.

https://doi.org/10.1371/journal.pone.0187894.t003

M1 and M2 macrophages in the infarcted myocardium of WT and AIM$^{-/-}$ mice

We evaluated macrophage accumulation in the infarcted myocardium after MI in WT and AIM$^{-/-}$ mice by immunohistology and RT-PCR. The number of MAC-3 positive cells indicating total macrophages in the infarcted myocardium was significantly lower in AIM$^{-/-}$ mice than in WT mice at 3 days after MI (Fig 3A and 3B).

Furthermore, we evaluated the number of M1 and M2 macrophages in the infarcted myocardium of WT and AIM$^{-/-}$ mice at 3 days after MI by double-staining immunofluorescence (Fig 4). The number of MAC-3/iNOS double-positive cells indicating M1 macrophages in the infarcted myocardium was significantly lower in AIM$^{-/-}$ mice than in WT

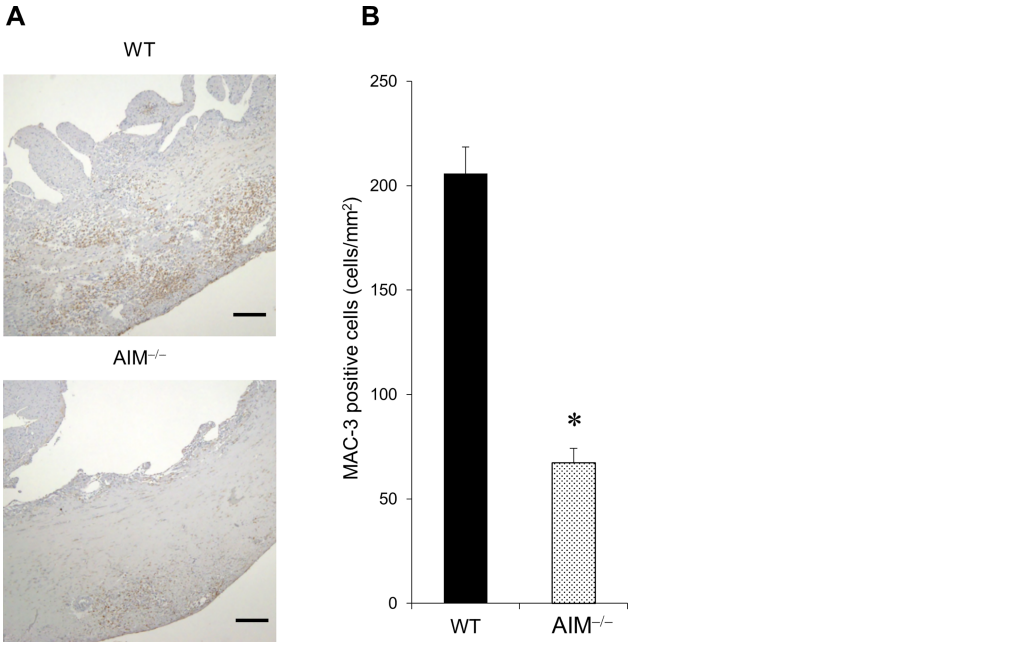

Fig 3. Macrophage accumulation in the infarcted myocardium of WT and AIM$^{-/-}$ mice. Representative images of immunohistochemical staining for MAC-3 positive cells in the infarcted myocardium of WT and AIM$^{-/-}$ mice at 3 days after MI **(A)**. The scale bars indicate 200 μm. The number of MAC-3 positive cells in the infarcted myocardium of WT and AIM$^{-/-}$ mice at 3 days after MI **(B)**. *P<0.05 compared with WT mice.

https://doi.org/10.1371/journal.pone.0187894.g003

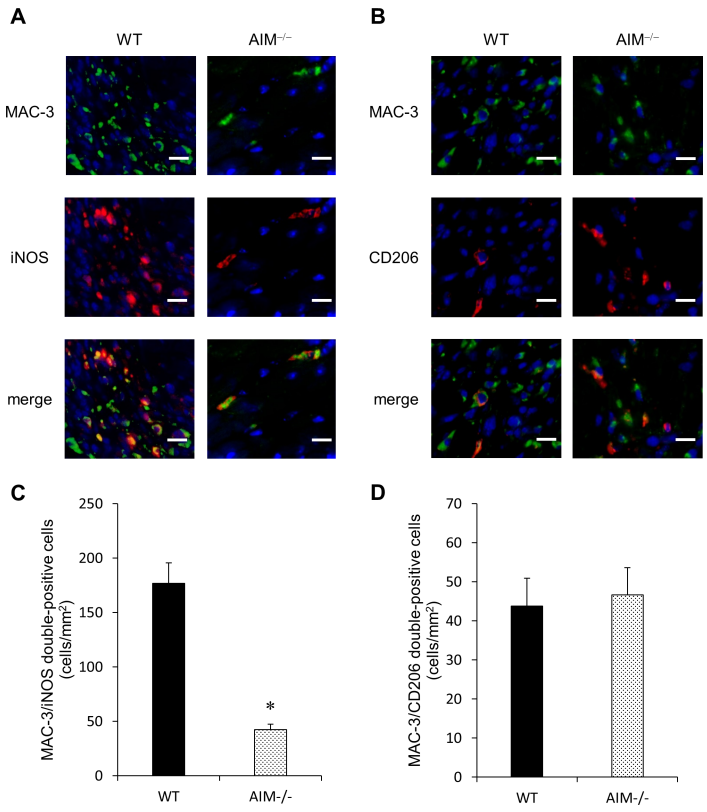

Fig 4. M1 and M2 macrophages in the infarcted myocardium of WT and AIM$^{-/-}$ mice at 3 days after MI. Representative images of immunofluorescence staining for MAC-3, iNOS (**A**) and CD206 (**B**). The number of MAC-3/iNOS double-positive cells (**C**) and MAC-3/CD206 double-positive cells (**D**) in the infarcted myocardium. * $P<0.05$ compared with WT mice.

https://doi.org/10.1371/journal.pone.0187894.g004

mice (Fig 4A and 4B). On the other hand, there was no significant difference in the number of MAC-3/CD206 double-positive cells indicating M2 macrophages between the two groups (Fig 4C and 4D). The mRNA levels of the indicated M1 macrophage markers (iNOS and IL-6) in the infarcted myocardium were significantly lower in AIM$^{-/-}$ mice than in WT mice at 3 days after MI (Fig 5A). The mRNA levels of IL-1β was also tended to be lower in AIM$^{-/-}$ mice. On the other hand, there was no significant difference in the mRNA levels of the indicated M2 macrophage markers (Arg-1, CD206 and TGF-β1) between WT and AIM$^{-/-}$ mice (Fig 5B). The mRNA levels of M1 and M2 macrophage markers in the infarcted myocardium at 7 days after MI were not significantly difference between WT and AIM$^{-/-}$ mice (Fig 5A and 5B).

Macrophage apoptosis in the infarcted myocardium of WT and AIM$^{-/-}$ mice at 3 days after MI

We evaluated that macrophage apoptosis in the infarcted myocardium of WT and AIM$^{-/-}$ mice at 3 days after MI (Fig 6A and 6B). The ratio of TUNEL/MAC-3 double-positive cells indicating apoptotic macrophages in total macrophages was significantly higher in AIM$^{-/-}$ mice than in WT mice.

On the other hand, there was no significant difference in the expression of MCP-1 in the infarcted myocardium at 3 days after MI between WT and AIM$^{-/-}$ mice (Fig 6C).

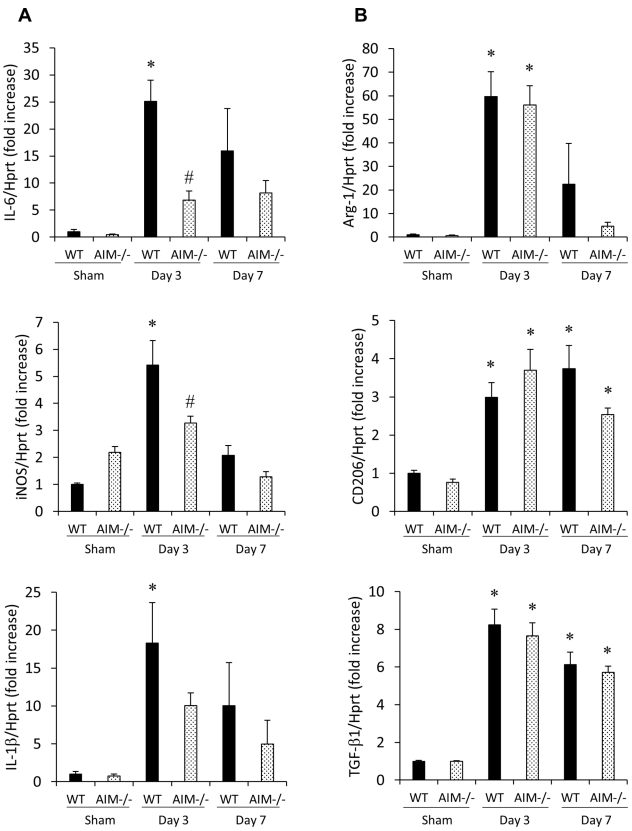

Fig 5. M1 and M2 macrophage marker expression levels in the infarcted myocardium of WT and AIM$^{-/-}$ mice. The mRNA levels of the indicated M1 (iNOS, IL-6 and IL-1β; **A**) and M2 (Arg-1, CD206 and TGF-β1; **B**) macrophage markers in the infarcted myocardium of WT and AIM$^{-/-}$ mice at 3 and 7 days after MI. **P*<0.05 compared with sham-operated WT mice, $^{\#}$*P*<0.05 compared with WT-MI mice, n = 7 per group.

https://doi.org/10.1371/journal.pone.0187894.g005

MMP-2 and 9 activity levels in the infarcted myocardium of WT and AIM$^{-/-}$ mice at 7 days after MI

We measured MMP-2 and 9 activity levels by gelatin zymography. As shown in Fig 7A–7C, there were no significant differences in MMP-2 or 9 activity levels in the myocardium between sham-operated WT and AIM$^{-/-}$ mice. In WT mice, both MMP-2 and MMP-9 activity levels in the infarcted myocardium were significantly higher than those in sham-operated myocardium. However, in AIM$^{-/-}$ mice, there were no significant differences in MMP-2 or 9 activity levels between the infarcted and sham-operated myocardium. Both MMP-2 and MMP-9 activity levels in the infarcted myocardium of AIM$^{-/-}$ mice were significantly lower than those of WT mice. We confirmed the molecular weight of MMP-2 and 9 by immunoblotting (S3 Fig).

Discussion

In this study, the survival rate of AIM$^{-/-}$ mice was significantly higher than that of WT mice in the acute phase after MI. Regarding the incidence of cardiac rupture, the rate of cardiac rupture was significantly lower in AIM$^{-/-}$ mice than in WT mice. The infarct size determined by the morphometric analysis of picrosirius red stained left ventricular cross-sections at 7 days after MI and the parameters measured by echocardiographic and hemodynamic analysis at 3 or 7 days after MI were comparable. Immunohistology and RT-PCR analysis showed the number of M1 macrophages and the expression levels of M1 markers (iNOS and IL-6) in the

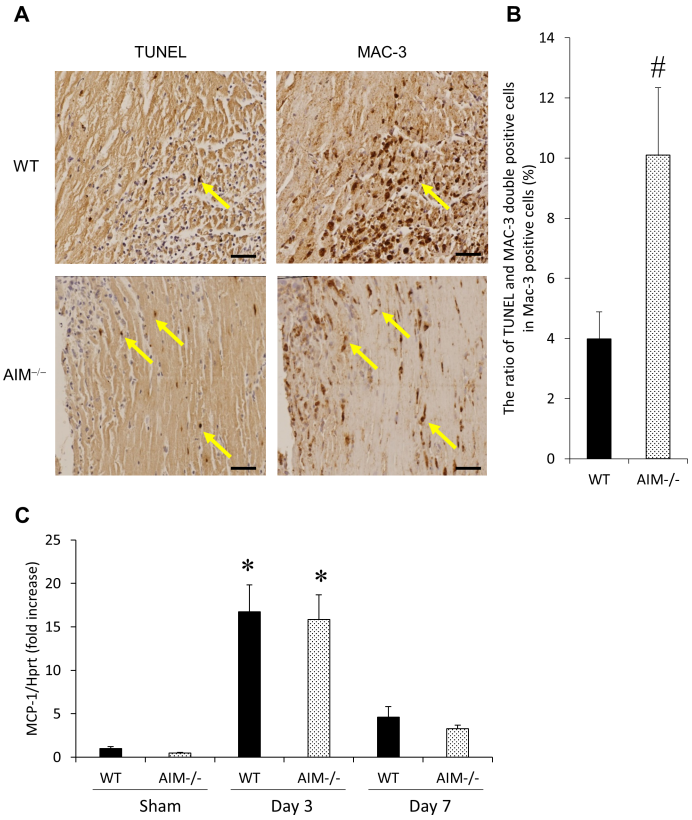

Fig 6. Macrophage apoptosis in the infarcted myocardium of WT and AIM$^{-/-}$ mice at 3 days after MI. Representative images of TUNEL/MAC-3 double-positive cells in the infarcted myocardium of WT and AIM$^{-/-}$ mice at 3 days after MI **(A)**. Mirror sections were stained for TUNEL and MAC-3, respectively and yellow arrows indicate TUNEL/MAC-3 double-positive cells. The ratio of TUNEL/MAC-3 double-positive cells in total MAC-3 positive cells in the infarcted myocardium of WT and AIM$^{-/-}$ mice at 3 days after MI **(B)**. The mRNA levels of MCP-1 in the infarcted myocardium of WT and AIM$^{-/-}$ mice at 3 and 7 days after MI (**C**). *P<0.05 compared with sham-operated WT mice, $^{\#}P$<0.05 compared with WT-MI mice. n = 6–7 per group.

https://doi.org/10.1371/journal.pone.0187894.g006

infarcted myocardium at 3 days after MI were significantly lower in AIM$^{-/-}$ mice than in WT mice. In contrast, there was no difference in the number of M2 macrophages and the expression of M2 markers (Arg-1, CD206 and TGF-β1) between the two groups. The ratio of apoptotic macrophages in total macrophages in the infarcted myocardium was significantly higher in AIM$^{-/-}$ mice than in WT mice at 3 days after MI. MMP-2 and 9 activity levels in the infarcted myocardium were significantly lower in AIM$^{-/-}$ mice than in WT mice at 7 days after MI.

AIM is a member of the scavenger receptor cysteine-rich superfamily [16]. It is secreted exclusively by macrophages and supports the survival of macrophages against various apoptosis-inducing stimuli [17, 18]. In addition to suppressing apoptosis, AIM promotes M1 monocyte/macrophage recruitment to inflamed tissues by facilitating MCP-1 expression [19, 20]. AIM contributes to macrophage accumulation in the inflamed tissue by maintaining survival and recruiting macrophages.

Although there are few studies about on cardiovascular disease, a recent study demonstrated that AIM contributed to the progression of adverse cardiac remodeling in the chronic phase after MI [31]. However, there is no study to reveal the role of AIM in the acute phase.

We demonstrated that AIM protein levels were increased after MI. Although, previous study reported the expression of AIM in the normal heart was very low [32], macrophages infiltrating into the infarcted myocardium might secrete AIM protein.

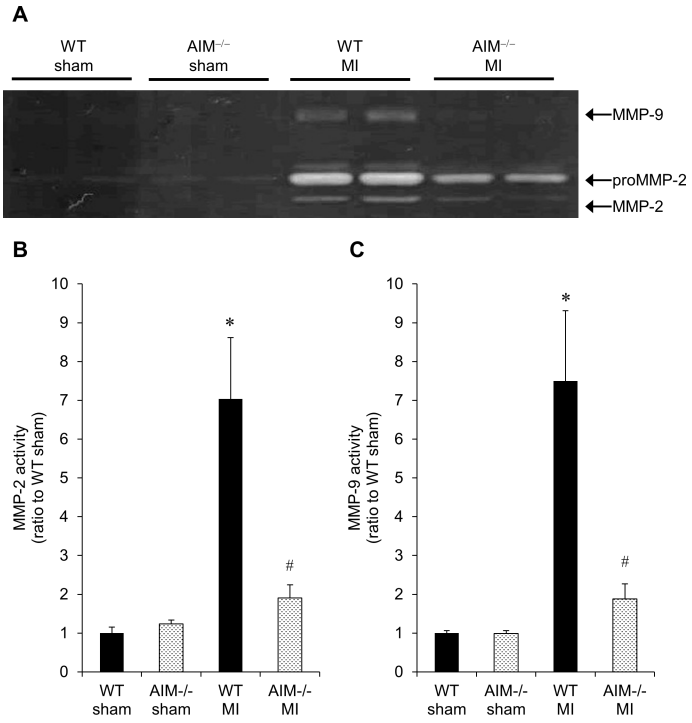

Fig 7. MMP-2 and 9 activity levels in the infarcted myocardium of WT and AIM$^{-/-}$ mice at 7 days after MI. A representative image of gelatin zymography (**A**), and quantitative analyses of MMP-2 (**B**) and 9 (**C**) activity levels in the infarcted myocardium of WT and AIM$^{-/-}$ mice at 7 days after MI. *P<0.05 compared with sham-operated WT mice, $^{\#}P$<0.05 compared with WT-MI mice, n = 6 per group.

https://doi.org/10.1371/journal.pone.0187894.g007

AIM depletion improved survival rates by reducing the incidence of cardiac rupture in the acute phase after MI. Although the risk factors for cardiac rupture are infarct size and blood pressure [33, 34], we demonstrated there was no difference in these parameters between WT and AIM$^{-/-}$ mice.

It was reported macrophage accumulation in the infarcted myocardium involved in cardiac rupture after MI [12, 13]. Macrophages play a pivotal role in cardiac remodeling after MI. Macrophages are grouped into the following two phenotypes (M1 and M2), the main functions of M1 macrophages include phagocytosis of cellular debris at sites of myocardial damage, secretion of inflammatory cytokines and reorganization of tissue matrices by producing metalloproteinases (MMPs) in the acute phase after MI [10, 11]. In contrast, M2 macrophages facilitate resolution of inflammation and regeneration by promoting myofibroblast accumulation, collagen deposition, and angiogenesis [12].

Because macrophage infiltration in the infarcted myocardium is peaks at 3–7 days after MI [23, 35, 36, 37], we evaluated it at 3 and 7 days after MI. Our data showed that the numbers of M1 macrophages and the expression levels of M1 markers, such as iNOS and IL-6 [10, 38, 39, 40], but not M2 markers, such as Arg-1, CD206 and TGF-β1 [9, 10, 38, 39], in the infarcted myocardium after MI were significantly lower in AIM$^{-/-}$ mice than in WT mice.

This phenomenon may be attributable to the following mechanism: AIM depletion may promote macrophage apoptosis in the infarcted myocardium, or suppress M1 macrophage recruitment by a decrease in MCP-1 expression.

In our study, the ratio of apoptotic macrophages in total macrophages in the infarcted myocardium was significantly higher in AIM$^{-/-}$ mice than in WT mice at 3 days after MI, whereas there was no significant difference in the expression of MCP-1 in the infarcted myocardium at

3 days after MI between WT and AIM$^{-/-}$ mice. These data suggested AIM depletion might suppress M1 macrophage accumulation in the infarcted myocardium through promoting macrophage apoptosis.

M1 macrophages are a potent source of MMP-2 and 9 in the acute phase after MI. MMP-9 is secreted mainly by neutrophils and M1 macrophages, and its activity peaks at 3 to 4 days after MI [35, 41, 42]. In contrast, MMP-2 is secreted mainly by fibroblasts and myofibroblasts, and its activity peaks at approximately 7 days after MI [35, 42]. However, M1 macrophages are also a potent source of MMP-2 [35, 43]. Although MMP-2 and 9 contribute to reorganization of tissue matrices in the acute phase after MI [10, 11], it has been suggested that excessive extracellular matrix degradation due to MMP activation may contribute to cardiac rupture after MI [38, 44].

In this study, the number of M1 macrophages and the activity levels of MMP-2 and 9 were significantly lower in AIM$^{-/-}$ mice than in WT mice in the infarcted myocardium in the acute phase after MI, indicating that AIM depletion may suppress the activity of MMP-2 and 9 by decreasing the levels of M1 macrophages, which are a potent source of MMP-2 and 9.

Conclusions

AIM depletion decreases the levels of M1 macrophages, which are a potent source of MMP-2 and 9, in the infarcted myocardium in the acute phase after MI by promoting macrophage apoptosis, and leads to a decrease in the incidence of cardiac rupture and improvements in survival rates.

Supporting information

S1 Fig. Immunoblotting for AIM in the infarcted myocardium of WT and AIM$^{-/-}$ mice at 7 days after MI.
(TIF)

S2 Fig. Representative images of picrosirius red-stained cardiac tissue sections of WT and AIM$^{-/-}$ mice at 7 days after MI.
(TIF)

S3 Fig. Representative images of zymography (A) and immunoblotting (B) for MMP-2 and 9 in the infarcted myocardium at 7 days after MI.
(TIF)

Acknowledgments

We thank Toru Miyazaki and Satoko Arai (Laboratory of Molecular Biomedicine for Pathogenesis, Center for Disease Biology and Integrative Medicine, Faculty of Medicine, University of Tokyo, Tockyo, Japan), Daisuke Nakano (Department of Pharmacology, Faculty of Medicine, Kagawa University, Kagawa, Japan), Yoshio Kushida and Toru Matsunaga (Department of Diagnostic Pathology, Kagawa University Hospital, Kagawa, Japan) for helpful advice. We also thank Teruyo Oka and Yoshiko Fujita (Department of Cardiorenal and Cerebrovascular Medicine, Faculty of Medicine, Kagawa University, Kagawa, Japan) for her excellent technical assistance. This research was supported by a Core Research for Evolutional Medical Science and Technology grant funded by the Agency for Medical Research and Development (AMED-CREST) (to Akira Nishiyama) and Grants-in-aid from the Ministry of Education, Culture, Sports, Science and Technology, Japan (to Tetsuo Minamino).

Author Contributions

Conceptualization: Shohei Ishikawa, Takahisa Noma, Takashi Matsuzaki, Makoto Ishizawa, Akira Nishiyama, Tetsuo Minamino.

Data curation: Shohei Ishikawa.

Formal analysis: Shohei Ishikawa, Hai Ying Fu, Naoki Nishimoto.

Funding acquisition: Takahisa Noma, Akira Nishiyama, Tetsuo Minamino.

Investigation: Shohei Ishikawa, Takahisa Noma, Hai Ying Fu, Takashi Matsuzaki, Kaori Ishikawa, Kazushi Murakami, Tetsuo Minamino.

Methodology: Shohei Ishikawa, Takahisa Noma, Hai Ying Fu, Takashi Matsuzaki, Makoto Ishizawa, Kaori Ishikawa, Kazushi Murakami, Tetsuo Minamino.

Project administration: Shohei Ishikawa, Takahisa Noma, Tetsuo Minamino.

Resources: Akira Nishiyama, Tetsuo Minamino.

Supervision: Takahisa Noma, Hai Ying Fu, Takashi Matsuzaki, Makoto Ishizawa, Kaori Ishikawa, Kazushi Murakami, Naoki Nishimoto, Akira Nishiyama, Tetsuo Minamino.

Validation: Shohei Ishikawa, Tetsuo Minamino.

Visualization: Shohei Ishikawa.

Writing – original draft: Shohei Ishikawa, Tetsuo Minamino.

Writing – review & editing: Shohei Ishikawa, Takahisa Noma, Naoki Nishimoto, Tetsuo Minamino.

References

1. Reed GW, Rossi J rey E, Cannon CP. Acute myocardial infarction. Lancet. 2016; 16: 30677–8. https://doi.org/10.1016/j.disamonth.2012.12.004 PMID: 23410669
2. Nichols M, Townsend N, Scarborough P, Rayner M, Lozano R, Naghavi M, et al. Cardiovascular disease in Europe 2014: epidemiological update. Eur Heart J. 2014; 35: 2950–9. https://doi.org/10.1093/eurheartj/ehu299 PMID: 25139896
3. Toru Takii, Satoshi Yasuda, Takahashi Jun, Kenta Ito, Nobuyuki Shiba, Shirato Kunio SH. Trends in Acute Myocardial Infarction Incidence and Mortality over 30 years in Japan. Circ J. 2010; 74: 93–100. PMID: 19942783
4. Yip H, Wu C, Chang H, Wang C-P, Cheng C-I, Chua S, et al. Cardiac rupture complicating acute myocardial infarction in the direct percutaneous coronary intervention reperfusion era. Chest. 2003; 124: 565–71. https://doi.org/10.1378/chest.124.2.565 PMID: 12907544
5. Honda S, Asaumi Y, Yamane T, Nagai T, Miyagi T, Noguchi T, et al. Trends in the Clinical and Pathological Characteristics of Cardiac Rupture in Patients With Acute Myocardial Infarction Over 35 Years. J Am Hear Assoc. 2014; 3: e000984. https://doi.org/10.1161/JAHA.114.000984 PMID: 25332178
6. Weinberger T, Schulz C. Myocardial infarction: A critical role of macrophages in cardiac remodeling. Frontiers in Physiology. 2015. https://doi.org/10.3389/fphys.2015.00107 PMID: 25904868
7. Frangogiannis NG. Regulation of the inflammatory response in cardiac repair. Circ Res. 2012; 110: 159–173. https://doi.org/10.1161/CIRCRESAHA.111.243162 PMID: 22223212
8. Fujiu K, Wang J, Nagai R. Cardioprotective function of cardiac macrophages. Cardiovascular Research. 2014. pp. 232–239. https://doi.org/10.1093/cvr/cvu059 PMID: 24675722
9. Troidl C, Möllmann H, Nef H, Masseli F, Voss S, Szardien S, et al. Classically and alternatively activated macrophages contribute to tissue remodelling after myocardial infarction. J Cell Mol Med. 2009; 13: 3485–3496. https://doi.org/10.1111/j.1582-4934.2009.00707.x PMID: 19228260
10. Ter Horst EN, Hakimzadeh N, Van Der Laan AM, Krijnen PAJ, Niessen HWM, Piek JJ. Modulators of macrophage polarization influence healing of the infarcted myocardium. International Journal of Molecular Sciences. 2015. pp. 29583–29591. https://doi.org/10.3390/ijms161226187 PMID: 26690421

11. Dutta P, Nahrendorf M. Monocytes in myocardial infarction. Arterioscler Thromb Vasc Biol. 2015; 35: 1066–1070. https://doi.org/10.1161/ATVBAHA.114.304652 PMID: 25792449

12. Nagai T, Honda S, Sugano Y, Matsuyama T aki, Ohta-Ogo K, Asaumi Y, et al. Decreased myocardial dendritic cells is associated with impaired reparative fibrosis and development of cardiac rupture after myocardial infarction in humans. J Am Heart Assoc. 2014; 3: 1–9. https://doi.org/10.1161/JAHA.114.000839 PMID: 24895162

13. van den Borne SWM, Cleutjens JPM, Hanemaaijer R, Creemers EE, Smits JFM, Daemen MJAP, et al. Increased matrix metalloproteinase-8 and -9 activity in patients with infarct rupture after myocardial infarction. Cardiovasc Pathol. Elsevier Inc.; 2009; 18: 37–43. https://doi.org/10.1016/j.carpath.2007.12.012 PMID: 18402833

14. Shiraishi M, Shintani Y, Shintani Y, Ishida H, Saba R, Yamaguchi A, et al. Alternatively activated macrophages determine repair of the infarcted adult murine heart. J Clin Invest. 2016; 126: 2151–2166. https://doi.org/10.1172/JCI85782 PMID: 27140396

15. Shiraishi M, Shintani Y, Shintani Y, Ishida H, Saba R, Yamaguchi A, et al. Alternatively activated macrophages determine repair of the infarcted adult murine heart. J Clin Invest. 2016; 126: 2151–66. https://doi.org/10.1172/JCI85782 PMID: 27140396

16. Kuwata K, Watanabe H, Jiang S-Y, Yamamoto T, Tomiyama-Miyaji C, Abo T, et al. AIM Inhibits Apoptosis of T Cells and NKT Cells in Corynebacterium-Induced Granuloma Formation in Mice. Am J Pathol. 2003; 162: 837–847. https://doi.org/10.1016/S0002-9440(10)63880-1 PMID: 12598318

17. Miyazaki T, Hirokami Y, Matsuhashi N, Takatsuka H, Naito M. Increased susceptibility of thymocytes to apoptosis in mice lacking AIM, a novel murine macrophage-derived soluble factor belonging to the scavenger receptor cysteine-rich domain superfamily. J Exp Med. 1999; 189: 413–422. https://doi.org/10.1084/jem.189.2.413 PMID: 9892623

18. Haruta I, Kato Y, Hashimoto E, Minjares C, Kennedy S, Uto H, et al. Association of AIM, a Novel Apoptosis Inhibitory Factor, with Hepatitis via Supporting Macrophage Survival and Enhancing Phagocytotic Function of Macrophages. J Biol Chem. 2001; 276: 22910–22914. https://doi.org/10.1074/jbc.M100324200 PMID: 11294859

19. Kurokawa J, Nagano H, Ohara O, Kubota N, Kadowaki T, Arai S, et al. Apoptosis inhibitor of macrophage (AIM) is required for obesity-associated recruitment of inflammatory macrophages into adipose tissue. Proc Natl Acad Sci U S A. 2011; 108: 12072–7. https://doi.org/10.1073/pnas.1101841108 PMID: 21730133

20. Antonio S, Mantovani A. Macrophage plasticity and polarization: in vivo veritas. J Clin Invest. 2012; 122: 787–795. https://doi.org/10.1172/JCI59643 PMID: 22378047

21. Hofmann U, Beyersdorf N, Weirather J, Podolskaya A, Bauersachs J, Ertl G, et al. Activation of CD4 + T lymphocytes improves wound healing and survival after experimental myocardial infarction in mice. Circulation. 2012; 125: 1652–1663. https://doi.org/10.1161/CIRCULATIONAHA.111.044164 PMID: 22388323

22. Arslan F, Smeets MB, Riem Vis PW, Karper JC, Quax PH, Bongartz LG, et al. Lack of fibronectin-EDA promotes survival and prevents adverse remodeling and heart function deterioration after myocardial infarction. Circ Res. 2011; 108: 582–592. https://doi.org/10.1161/CIRCRESAHA.110.224428 PMID: 21350212

23. Anzai A., Anzai T, Nagai S, Maekawa Y, Naito K, Kaneko H, et al. Regulatory Role of Dendritic Cells in Postinfarction Healing and Left Ventricular Remodeling. Circulation. 2012; 125: 1234–1245. https://doi.org/10.1161/CIRCULATIONAHA.111.052126 PMID: 22308302

24. Foster CR, Daniel LL, Daniels CR, Dalal S, Singh M, Singh K. Deficiency of Ataxia Telangiectasia Mutated Kinase Modulates Cardiac Remodeling Following Myocardial Infarction: Involvement in Fibrosis and Apoptosis. PLoS One. 2013; 8: 1–11. https://doi.org/10.1371/journal.pone.0083513 PMID: 24358288

25. Okada H, Takemura G, Kosai K, Tsujimoto A, Esaki M, Takahashi T, et al. Combined therapy with cardioprotective cytokine administration and antiapoptotic gene transfer in postinfarction heart failure. Am J Phyiol Hear Circ Physiol. 2009; 296: 616–626. https://doi.org/10.1152/ajpheart.01147.2008 PMID: 19151252

26. Oshima E, Ishihara T, Yokota O, Nakashima-yasuda H, Nagao S. Accelerated Tau Aggregation, Apoptosis and Neurological Dysfunction Caused by Chronic Oral Administration of Aluminum in a Mouse Model of Tauopathies. Brain Patholoby. 2013; 23: 633–644. https://doi.org/10.1111/bpa.12059 PMID: 23574527

27. Li GH, Shi Y, Chen Y, Sun M, Sader S, Maekawa Y, et al. Gelsolin regulates cardiac remodeling after myocardial infarction through DNase I-mediated apoptosis. Circ Res. 2009; 104: 896–904. https://doi.org/10.1161/CIRCRESAHA.108.172882 PMID: 19246681

28. Everaert BR, Boulet GA, Timmermans J, Vrints CJ. Importance of Suitable Reference Gene Selection for Quantitative Real-Time PCR: Special Reference to Mouse Myocardial Infarction Studies. PLoS One. 2011; 6. https://doi.org/10.1371/journal.pone.0023793 PMID: 21858224

29. Fu HY, Okada K, Liao Y. Ablation of C / EBP Homologous Protein Attenuates Endoplasmic Reticulum–Mediated Apoptosis and Cardiac. Circulation. 2010; 122: 361–9. https://doi.org/10.1161/CIRCULATIONAHA.109.917914 PMID: 20625112

30. Van Craeyveld E, Jacobs F, Gordts SC, De Geest B. Low-density lipoprotein receptor gene transfer in hypercholesterolemic mice improves cardiac function after myocardial infarction. Gene Ther. Nature Publishing Group; 2012; 19: 860–871. https://doi.org/10.1038/gt.2011.147 PMID: 21975462

31. Nishikido T, Oyama J-I, Shiraki A, Komoda H, Node K. Deletion of Apoptosis Inhibitor of Macrophage (AIM)/CD5L Attenuates the Inflammatory Response and Infarct Size in Acute Myocardial Infarction. J Am Heart Assoc. 2016; 5: e002863. https://doi.org/10.1161/JAHA.115.002863 PMID: 27045005

32. Tomura S, Uchida M, Yonezawa T, Kobayashi M, Bonkobara M. Molecular Cloning and Gene Expression of Canine Apoptosis Inhibitor of Macrophage. J Vet Med Sci. 2014; 76: 1641–5. https://doi.org/10.1292/jvms.14-0166 PMID: 25649949

33. Christensen Danis J., Ford Marilyn, James Reading C. Hilmon Castle Effect of Hypertension on Myocardial Rupture after Acute Myocardial Infarction. Chest 1977; 72: 618–22 https://doi.org/10.1378/chest.72.5.618 PMID: 913141

34. Barandon L, Couffinhal T, Ezan J, Dufourcq P, Costet P, Alzieu P, et al. Reduction of Infarct Size and Prevention of Cardiac Rupture in Transgenic Mice Overexpressing FrzA. Circulation. 2003; 108: 2282–2290. https://doi.org/10.1161/01.CIR.0000093186.22847.4C PMID: 14581414

35. Tao Z-Y, Cavasin MA, Yang F, Liu Y-H, Yang X-P. Temporal changes in matrix metalloproteinase expression and inflammatory response associated with cardiac rupture after myocardial infarction in mice. Life Sci. 2004; 74: 1561–1572. https://doi.org/10.1016/j.lfs.2003.09.042 PMID: 14729404

36. Hayashidani S, Tsutsui H, Shiomi T, Ikeuchi M, Matsusaka H, Suematsu N, et al. Anti-Monocyte Chemoattractant Protein-1 Gene Therapy Attenuates Left Ventricular Remodeling and Failure After Experimental Myocardial Infarction. Circulation. 2003; 108: 2134–2140. https://doi.org/10.1161/01.CIR.0000092890.29552.22 PMID: 14517168

37. Nahrendorf M, Pittet MJ, Swirski FK. Monocytes: Protagonists of infarct inflammation and repair after myocardial infarction. Circulation. 2010; 121: 2437–2445. https://doi.org/10.1161/CIRCULATIONAHA.109.916346 PMID: 20530020

38. White DA, Su Y, Kanellakis P, Kiriazis H, Morand EF, Bucala R, et al. Differential roles of cardiac and leukocyte derived macrophage migration inhibitory factor in inflammatory responses and cardiac remodelling post myocardial infarction. J Mol Cell Cardiol. 2014; 69: 32–42. https://doi.org/10.1016/j.yjmcc.2014.01.015 PMID: 24508700

39. Forbes SJ, Rosenthal N. Preparing the ground for tissue regeneration: from mechanism to therapy. Nat Med. 2014; 20: 857–69. https://doi.org/10.1038/nm.3653 PMID: 25100531

40. Zhou L-S, Zhao G-L, Liu Q, Jiang S-C, Wang Y, Zhang D-M. Silencing collapsin response mediator protein-2 reprograms macrophage phenotype and improves infarct healing in experimental myocardial infarction model. J Inflamm (Lond). 2015; 12: 11. https://doi.org/10.1186/s12950-015-0053-8 PMID: 25685072

41. Lambert JM, Lopez EF, Lindsey ML. Macrophages role following myocardial infarction. Int J Cardiol. 2008; 130: 147–158. https://doi.org/10.1016/j.ijcard.2008.04.059 PMID: 18656272

42. Chen J. Near-Infrared Fluorescent Imaging of Matrix Metalloproteinase Activity After Myocardial Infarction. Circulation. 2005; 111: 1800–1805. https://doi.org/10.1161/01.CIR.0000160936.91849.9F PMID: 15809374

43. Vanhoutte D, Schellings M, Pinto Y, Heymans S. Relevance of matrix metalloproteinases and their inhibitors after myocardial infarction: A temporal and spatial window. Cardiovasc Res. 2006; 69: 604–613. https://doi.org/10.1016/j.cardiores.2005.10.002 PMID: 16360129

44. Matsumura SI, Iwanaga S, Mochizuki S, Okamoto H, Ogawa S, Okada Y. Targeted deletion or pharmacological inhibition of MMP-2 prevents cardiac rupture after myocardial infarction in mice. J Clin Invest. 2005; 115: 599–609. https://doi.org/10.1172/JCI22304 PMID: 15711638